Supplementary Information

Unconventional hidden Rashba effects in two-dimensional InTe

Sangmin Lee[1], Miyoung Kim[1], and Young-Kyun Kwon[2,*]

[1]*Department of Materials Science & Engineering and Research Institute of Advanced Materials, Seoul National University, 08826, Seoul, South Korea*

[2]*Department of Physics, Department of Information Display, and Research Institute for Basic Sciences, Kyung Hee University, 024447, Seoul, South Korea*

**Corresponding author. E-mail: ykkwon@khu.ac.kr*

Supplementary Note 1

We developed a straightforward model Hamiltonian that explicitly accounts for two sets of R-2 bands in addition to Rashba splitting and the sublayer-sublayer (SL-SL) interaction in order to better understand the unconventional hidden Rashba (R-2) effect. This approach is essentially the same as that described in [9] in the main text's Reference section.

For the model Hamiltonian, eight bases $\{|T,a,\uparrow\rangle, |T,a,\downarrow\rangle, |B,a,\uparrow\rangle, |B,a,\downarrow\rangle, |T,b,\uparrow\rangle, |T,b,\downarrow\rangle, |B,b,\uparrow\rangle, |B,b,\downarrow\rangle\}$ are employed to describe states of electrons at top (T) and bottom (B) SLs with spin up ($\uparrow$) and down ($\downarrow$). Furthermore, since unconventional hidden Rashba effect needs two sets of R-2 bands, we labeled the corresponding sets by a and b. Also, we consider a Hamiltonian $\mathcal{H} = \mathcal{H}_0 + \mathcal{H}_R + \mathcal{H}_I$, which encompasses the free ($\mathcal{H}_0$), Rashba ($\mathcal{H}_R$), SL-SL interaction ($\mathcal{H}_I$) part. The free part is given by $-\frac{\hbar^2 k^2}{2m_a^*}$ and $-\frac{\hbar^2 k^2}{2m_b^*}$ where k is crystal momentum, and m_a^* and m_b^* are effective masses for R-2 pair a and b, respectively.

Since the top and bottom SLs carry opposite local dipole moments, the Rashba splitting $\mathcal{H}_R$ is given by

$$\langle T,a,\uparrow|\mathcal{H}_R|T,a,\uparrow\rangle = -\alpha_R^a k \qquad \langle T,a,\downarrow|\mathcal{H}_R|T,a,\downarrow\rangle = \alpha_R^a k$$

$$\langle B,a,\uparrow|\mathcal{H}_R|B,a,\uparrow\rangle = \alpha_R^a k \qquad \langle B,a,\downarrow|\mathcal{H}_R|B,a,\downarrow\rangle = -\alpha_R^a k \tag{1}$$

where α_R^a is Rashba strength for R-2 pair a. Equivalent terms are given for R-2 pair b with Rashba strength α_R^b. Also, we expand SL-SL interaction $\mathcal{H}_I$ up to the 2nd order and represent them as

$$\langle T,a,\uparrow|\mathcal{H}_R|B,a,\uparrow\rangle = E_{I,a}^0 + E_{I,a}^1 k^2 \qquad \langle T,a,\downarrow|\mathcal{H}_R|B,a,\downarrow\rangle = E_{I,a}^0 + E_{I,a}^1 k^2$$

$$\langle T,b,\uparrow|\mathcal{H}_R|B,b,\uparrow\rangle = E_{I,b}^0 + E_{I,b}^1 k^2 \qquad \langle T,b,\downarrow|\mathcal{H}_R|B,b,\downarrow\rangle = E_{I,b}^0 + E_{I,b}^1 k^2 \tag{2}$$

Then with the $\{|T,a,\uparrow\rangle, |T,b,\uparrow\rangle, |B,a,\uparrow\rangle, |B,b,\uparrow\rangle, |T,a,\downarrow\rangle, |T,b,\downarrow\rangle, |B,a,\downarrow\rangle, |B,b,\downarrow\rangle\}$ basis order, the model Hamiltonian has a block diagonal form $\begin{pmatrix} \mathcal{H}_U & 0 \\ 0 & \mathcal{H}_D \end{pmatrix}$ where the eigenvalues of the block matrix $\mathcal{H}_U$ are degenerate with those of $\mathcal{H}_D$. Thus, we only need to solve $\mathcal{H}_U$ matrix which is given by

$$\mathcal{H}_U = \begin{pmatrix} -\frac{\hbar^2 k^2}{2m_a^*} - \alpha_R^a k & 0 & E_{I,a}^0 + E_{I,a}^1 k^2 & 0 \\ 0 & -\frac{\hbar^2 k^2}{2m_b^*} - \alpha_R^b k & 0 & E_{I,b}^0 + E_{I,b}^1 k^2 \\ E_{I,a}^0 + E_{I,a}^1 k^2 & 0 & -\frac{\hbar^2 k^2}{2m_a^*} + \alpha_R^a k & 0 \\ 0 & E_{I,b}^0 + E_{I,b}^1 k^2 & 0 & -\frac{\hbar^2 k^2}{2m_b^*} + \alpha_R^b k \end{pmatrix} \tag{3}$$

whose eigenvalues are given by

$$E_{a,\pm} = -\frac{\hbar^2 k^2}{2m_a^*} \pm \sqrt{(\alpha_R^a k)^2 + (E_{I,a}^0 + E_{I,a}^1 k^2)^2} \quad \text{and} \quad E_{b,\pm} = -\frac{\hbar^2 k^2}{2m_b^*} \pm \sqrt{(\alpha_R^b k)^2 + (E_{I,b}^0 + E_{I,b}^1 k^2)^2}, \tag{4}$$

which describe four doubly degenerate bands.

In order to determine the parameters in Eq. (4), we fitted the four Rashba bands (VB2 ~ VB5) computed by our first-principles calculation results shown in Fig. 4 in the main text. The results are summarized in Figure S6 in the Supplementary Information.

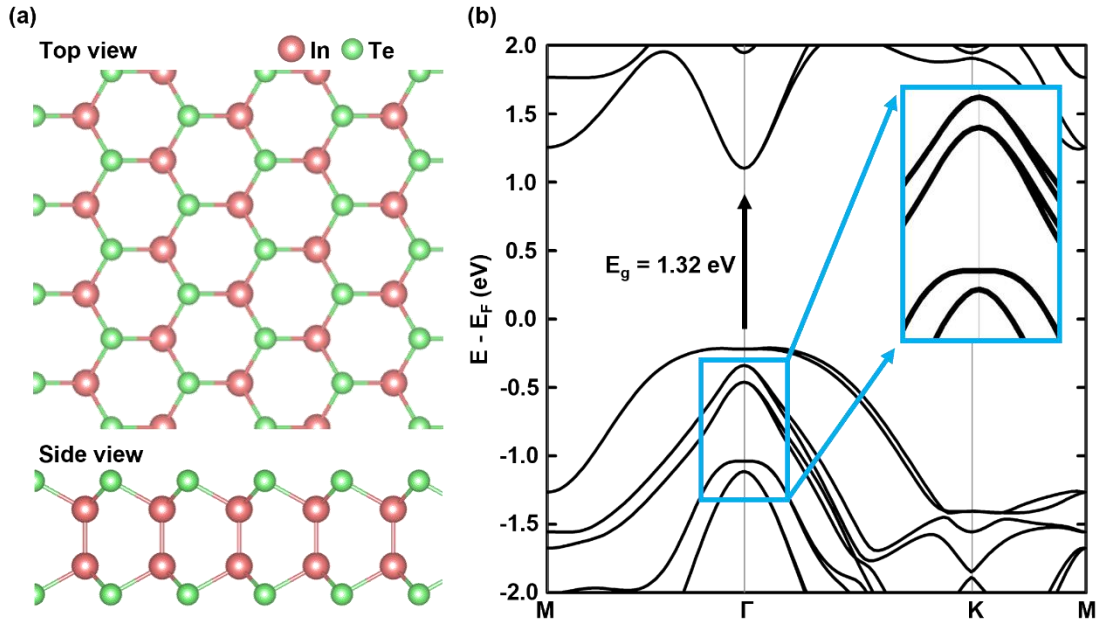

Supplementary Figure 1 (a) Top and side view of the crystal structure of monolayer InTe with mirror symmetry. (b) Its electronic band structures, of which a couple of valence bands near the Γ point are shown in insets. The mirror phase has a band gap of 1.32 eV at the Γ point. The breaking of inversion symmetry in the mirror phase lifts the spin degeneracy.

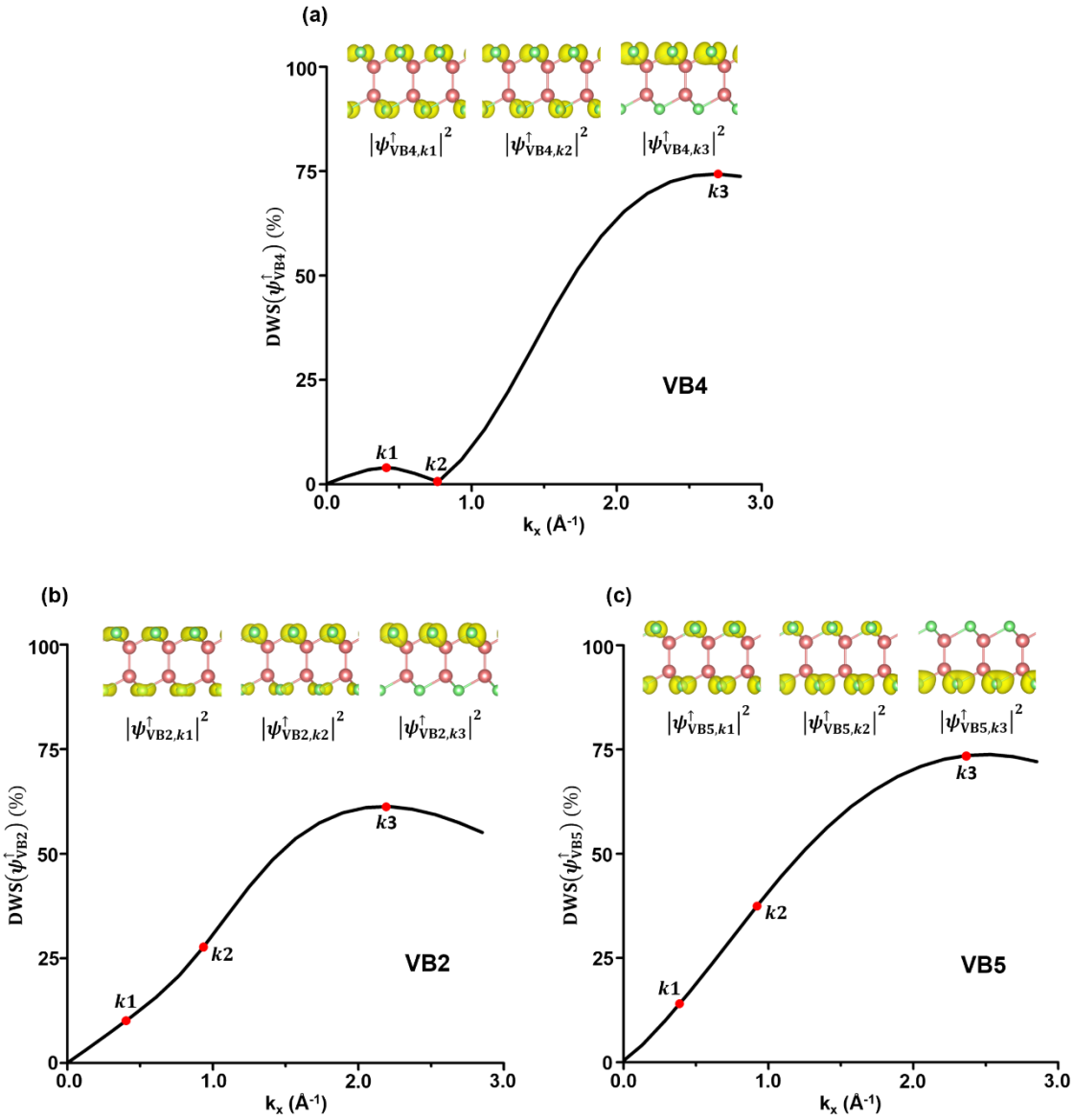

Supplementary Figure 2 Degree of wavefunction segregation (DWS) of InTe monolayer with inversion evaluated for spin up in (a) VB4, (b) VB2, and (c) VB5 along $\mathbf{k}_{\Gamma-\mathrm{K}}$. The insets show the wavefunctions squared at three different $\mathbf{k}$ points, $k1$, $k2$, and $k3$. Like in VB3 shown in Fig. 2(g) of the main text, there exists the transition of wavefunction segregation in VB4. Contrary to these two bands, the DWS of VB2 and VB5 do not show such a transition, but smooth shapes without singular points. Thus, the transition of SLL occurs only in VB3 and VB4.

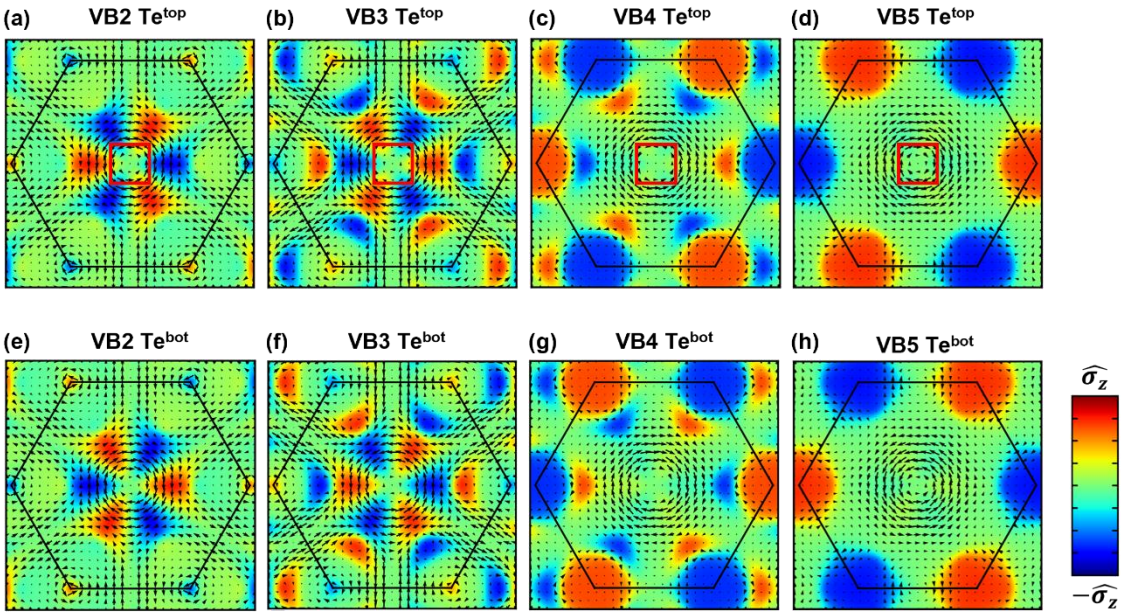

Supplementary Figure 3 Spatially resolved spin maps on the top (a-d) and bottom (e-h) Te atom layer plotted in the first Brillouin zone for VB2 ~ VB5. The size of the black arrows and different colors indicate the in-plane and out-of-plane spin components. The opposite spin polarizations in each band are spatially separated into top and bottom Te layers resulting in SLL. The spin textures displayed in Figs. 3(a-d) of the main text were plotted in the regions indicated by red boxes in (a-d).

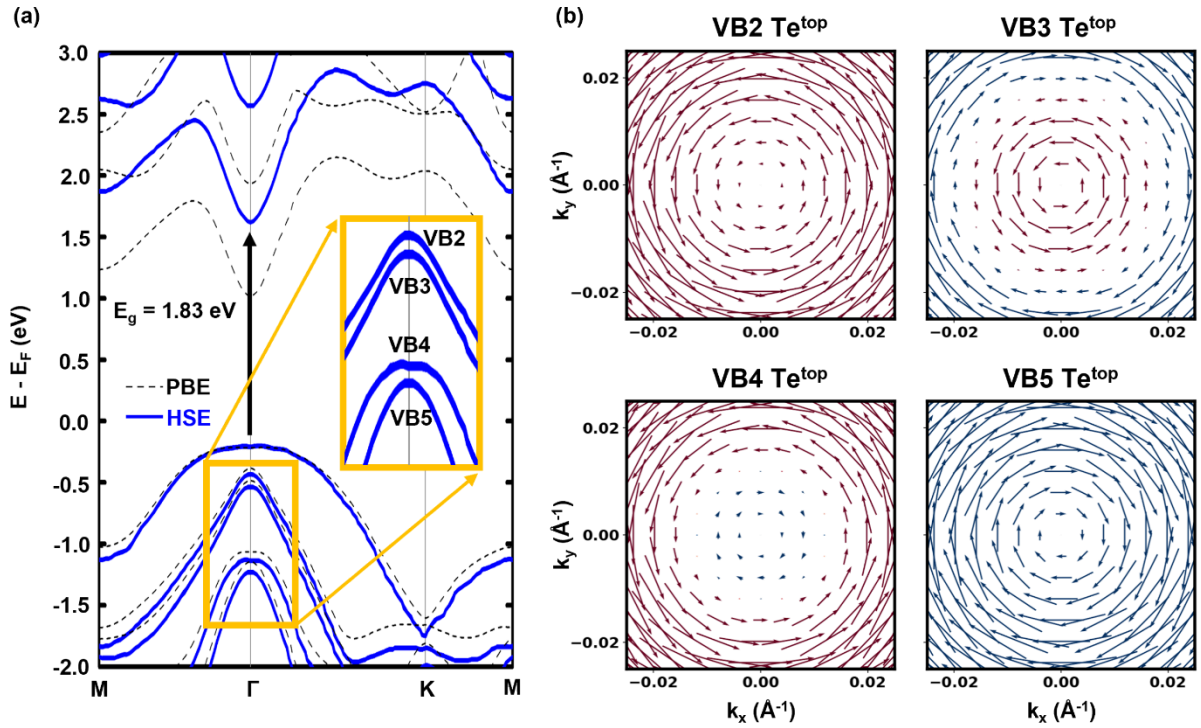

Supplementary Figure 4 Electronic band structures and spin textures of InTe calculated by HSE06 functional. (a) The calculated band gap values at the Γ point is 1.83 eV, which is 0.6eV larger than PBE result. Four Rashba bands are indicated in the inset. (b) Spatially resolved spin texture of Rashba bands (VB2 ~ VB5) projected onto top Te sublayers. It shows the same spin helicity as the PBE result.

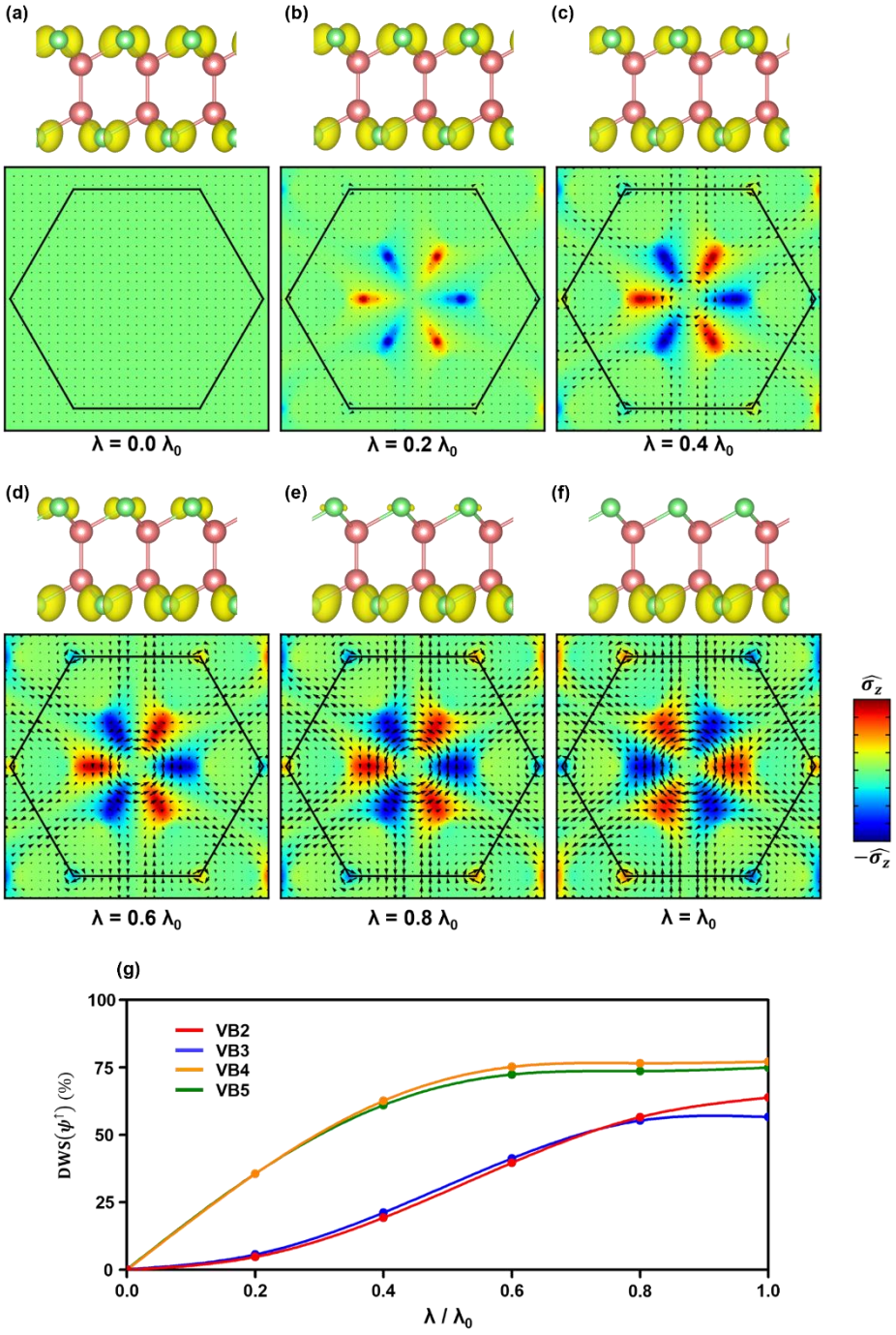

Supplementary Figure 5 Evolution of the spin-layer locking with the SOC strength $\lambda/\lambda_0 \in (0,1)$, where λ_0 is the real SOC strength. (a-f) Spin-resolved wavefunctions squared, $\left|\psi^{\uparrow}_{\mathrm{VB2},\mathbf{k}}\right|^2$, calculated at $\mathbf{k}_{\Gamma-\mathrm{M}} = (0, 0.15)(2\pi/a)$ near the Γ point and spatially resolved spin maps on the top Te atom layer plotted in the first Brillouin zone for VB2 with different λ values. The size of the black arrows and different colors indicate the in-plane and out-of-plane spin components. (g) Degree of wavefunction segregation (DWS) evaluated for spin up at each band as a function of λ.

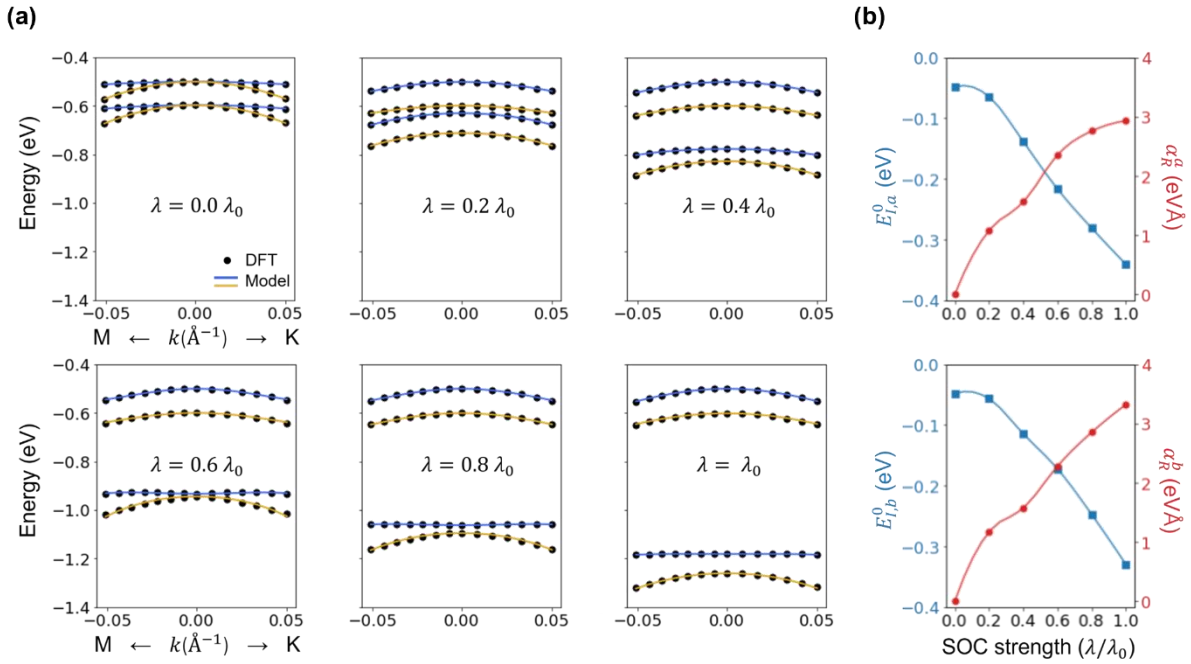

Supplementary Figure 6 Four Rashba bands (VB2~ VB5) near the Γ point. (a) The model specified in Eq. (4) was fitted using the energy eigenvalues determined by DFT, which are represented by the black circle dots. Blue and yellow solid lines show the model-fitted eigenvalues with two pairs of R-2 bands, respectively. (b) The fitted values of the interaction energy (E_I^0) and the Rashba strength (α_R) as a function of SOC strength (λ).